Partanen, Mikko; Tulkki, Jukka

Design of an experimental setup for the measurement of light-driven atomic mass density waves in a silicon crystal

Published in:
Optical Trapping and Optical Micromanipulation XVI

DOI:
10.1117/12.2529138

Published: 01/01/2019

Document Version
Publisher's PDF, also known as Version of record

Design of an experimental setup for the measurement of light-driven atomic mass density waves in a silicon crystal

Mikko Partanen, Jukka Tulkki

Mikko Partanen, Jukka Tulkki, "Design of an experimental setup for the measurement of light-driven atomic mass density waves in a silicon crystal," Proc. SPIE 11083, Optical Trapping and Optical Micromanipulation XVI, 1108329 (9 September 2019); doi: 10.1117/12.2529138

Event: SPIE Nanoscience + Engineering, 2019, San Diego, California, United States

Design of an experimental setup for the measurement of light-driven atomic mass density waves in a silicon crystal

Mikko Partanen[1,2] and Jukka Tulkki[3]

[1]Photonics Group, School of Electrical Engineering, Aalto University, P.O. Box 15500, 00076 Aalto, Finland

[2]Photonic Device Physics Laboratory, College of Science, Yonsei University, 50 Yonsei-ro, Seodaemun-gu, Seoul 03722, Korea

[3]Engineered Nanosystems Group, School of Science, Aalto University, P.O. Box 12200, 00076 Aalto, Finland

ABSTRACT

The recently introduced mass-polariton (MP) theory of light describes light in a medium as a coupled state of the field and matter [Phys. Rev. A 95, 063850 (2017)]. In the MP theory, the optical force density drives forward an atomic mass density wave (MDW) that accompanies electromagnetic waves in a medium. The MDW is necessary for the fulfilment of the conservation laws and the Lorentz covariance of light. In silicon at wavelength $\lambda_0 = 1550$ nm, the atomic MDW carries 92% of the total momentum and angular momentum of light. The MDW of a light pulse having field energy E propagating in a dielectric also transfers a net mass equal to $\delta M = (n_\mathrm{p}n_\mathrm{g} - 1)E/c^2$, where n_p and n_g are the phase and group refractive indices. In this work, we present a schematic experimental setup for the measurement of the MDW in a silicon crystal. This setup overcomes many challenges that have been present in previously introduced setups and that have made the experimental observation of the MDW effect difficult due to its smallness in comparison with other effects, such as the momentum transfer by absorption and reflections. The present setup also overcomes challenges with elastic relaxation effects while extending possible measurement time scales beyond the time scale of sound waves in the setup geometry. For the proposed setup, we also compare the predictions of the MP theory of light to the predictions of the conventional Minkowski theory, where the total momentum of light is carried by the electromagnetic field. We also aim at optimizing experimental studies of the MDW effect using the proposed setup.

Keywords: mass-polariton, mass density wave, optical shock wave, electrodynamics, optomechanics

1. INTRODUCTION

The momentum and angular momentum of light continue to be subject of intense research as demonstrated by recent investigations of these quantities in vacuum,[1,2] in photonic materials,[3–6] in the near-field regime,[7–10] and also in the quantum domain.[11] In the case of continuous media, the experiments studying the momentum transfer between the electromagnetic field and the medium have mainly focused on the interaction of light with liquids.[12–18] However, some recent experiments have also investigated mechanical effects of the momentum transfer of light in solids.[19,20] In the recent experiments by Požar *et al.*,[19,20] the small elastic waves of atoms generated by light reflected from a mirror were experimentally measured. The extremely small amplitude elastic waves waves (amplitudes of the order of picometers) were detected by a piezoelectric sensor. The elastic waves were, however, generated by the optical force caused by the reflection of a laser beam from a metal-coated dielectric. We suggest that this experimental approach could also be applied to discover elastic waves resulting from intra-material optical forces like the Abraham force of the light pulse propagating inside the dielectric. The displacements generated by the optical force have the largest amplitude inside the dielectric, but in the same way as in the experiment of Požar *et al.*, the elastic waves resulting from the relaxation of these displacements will propagate to the surface and could be detected there using the same piezoelectric approach.

The discovery by Požar *et al.* and various observations made with liquids are special cases of a general phenomenology of atomic density waves that are generated by the optical force when light is partially reflected from and partially transmitted through a dielectric. Fundamental and unified understanding of the dynamics

Optical Trapping and Optical Micromanipulation XVI, edited by Kishan Dholakia, Gabriel C. Spalding, Proc. of SPIE Vol. 11083, 1108329 · © 2019 SPIE
CCC code: 0277-786X/19/$21 · doi: 10.1117/12.2529138

of these atomic density waves is only possible by the mass-polariton (MP) theory of light developed by us recently.[21–26] The MP theory combines the optical and elastic forces on equal footing and enables solving the dynamical equation for the atoms in a dielectric. Thus, the MP theory of light combines Maxwell's equations of the field with the Newtonian mechanics of the medium[21] and allows detailed optoelastic continuum dynamics (OCD) simulations studying the coupled dynamics of the field and the medium. The MP theory shows that light in a medium is associated with an atomic mass density wave (MDW) that is necessary for the fulfillment of conservation laws and the Lorentz covariance of light. The MDW also carries a major part of the total linear and angular momenta of light in many common dielectrics. For example, in silicon at wavelength $\lambda_0 = 1550$ nm, the atomic MDW carries 92% of the total momentum and angular momentum of light. The classical field-theoretical background and Lorentz covariance properties of the MP theory of light are presented in detail in recent works.[25,26]

In this work, we first review the foundations of the MP theory and its numerical implementation using the OCD model. Then we present a schematic experimental setup for the observation of a small displacement of atoms in a silicon crystal as a result of the optical force. The new experimental arrangement, which will be discussed in detail below, overcomes many challenges that are present in previously introduced experimental setups.[22,23,27–29] We also perform OCD simulations of the field-medium dynamics in the setup especially concentrating on the transient field effects of switching on the laser. The simulations also aim at optimizing experimental studies of the atomic MDW dynamics in solids.

2. OPTOELASTIC CONTINUUM DYNAMICS

2.1 Optical and elastic forces and Newton's equation of motion

The classical field-theoretical background of the MP theory of light is presented in detail in Refs.,[25,26] which complement the previous studies of the MP theory of light initiated in Refs.[21,22] In the MP theory, the dynamics of the field and the matter are coupled through Newton's equation of motion, which accounts for the optical and elastic forces on equal footing. In the laboratory frame, which is an inertial frame, where the medium is at rest in the absence of light, Newton's equation of motion for the mass density $\rho_{\mathrm{a}}(\mathbf{r},t)$ of the medium and the instantaneous position- and time-dependent displacement field $\mathbf{r}_{\mathrm{a}}(\mathbf{r},t)$ of atoms is written in the nonrelativistic limit as[21]

$$\rho_{\mathrm{a}}(\mathbf{r},t)\frac{d^2\mathbf{r}_{\mathrm{a}}(\mathbf{r},t)}{dt^2} = \mathbf{f}_{\mathrm{opt}}(\mathbf{r},t) + \mathbf{f}_{\mathrm{el}}(\mathbf{r},t). \tag{1}$$

Here $\mathbf{f}_{\mathrm{opt}}(\mathbf{r},t)$ is the optical force density that the atoms experience due to the electromagnetic field and $\mathbf{f}_{\mathrm{el}}(\mathbf{r},t)$ is the elastic force density, which arises between atoms that are displaced from their original equilibrium positions by the optical force. For anisotropic cubic crystals, such as silicon that is used in the setup presented in this work, the well-known elastic force density is given in Ref.[30]

The optical force density in the MP theory of light in a lossless dispersive dielectric is presented in Ref.[22] The extension of this force density for lossy dielectrics is presented in Ref.[29] as

$$\mathbf{f}_{\mathrm{opt}} = \underbrace{\rho_{\mathrm{e}}\mathbf{E} + \mu_0\mathbf{J}\times\mathbf{H}}_{\mathbf{f}_{\mathrm{L}}}\underbrace{-\varepsilon_0 n_{\mathrm{g}}\mathbf{E}^2\nabla n_{\mathrm{p}}}_{\mathbf{f}_{\mathrm{int}}}\underbrace{+\frac{n_{\mathrm{p}}n_{\mathrm{g}}-1}{c^2}\frac{\partial}{\partial t}\mathbf{E}\times\mathbf{H}}_{\mathbf{f}_{\mathrm{A}}}. \tag{2}$$

Here ρ_{e} is the free electric charge density of the medium, n_{p} is the phase refractive index, n_{g} is the group refractive index, and $\mathbf{J} = \sigma\mathbf{E}$ is the free current density, where $\sigma = \varepsilon_{\mathrm{i}}\omega$ is the electrical conductivity with ε_{i} the imaginary part of the permittivity. In Eq. (2), the term $\mathbf{f}_{\mathrm{L}}$ is the Lorentz force on free charges and currents, which leads to damping of the field inside lossy media, the term $\mathbf{f}_{\mathrm{int}}$ is the interface force, which is related to the changes of the refractive index, and the term $\mathbf{f}_{\mathrm{A}}$ is the Abraham force, which drives in a medium forward an atomic MDW as shown in Refs.[21–24]

2.2 Momentum and angular momentum of the coupled field-medium state of light

In the MP theory of light, the total momentum and angular momentum of the coupled state of light is shared between the electromagnetic field and the atomic MDW. The total momentum of the coupled MP state and its field and the medium contributions are given by integrals of classical momentum densities of the field and the medium as

$$\mathbf{p}_{\mathrm{MP}} = \int \Big(\frac{\mathbf{E}\times\mathbf{H}}{c^2} + \rho_{\mathrm{a}}\mathbf{v}_{\mathrm{a}}\Big) d^3r, \tag{3}$$

$$\mathbf{p}_{\mathrm{field}} = \int \frac{\mathbf{E}\times\mathbf{H}}{c^2} d^3r, \qquad \mathbf{p}_{\mathrm{MDW}} = \int \rho_{\mathrm{a}}\mathbf{v}_{\mathrm{a}} d^3r. \tag{4}$$

Correspondingly, the total angular momentum of the coupled state of light and its field and the MDW contributions are given by integrals of the well-known classical expressions of the angular momentum densities of the field and the medium as

$$\mathbf{J}_{\mathrm{MP}} = \int \mathbf{r}\times\Big(\frac{\mathbf{E}\times\mathbf{H}}{c^2} + \rho_{\mathrm{a}}\mathbf{v}_{\mathrm{a}}\Big) d^3r, \tag{5}$$

$$\mathbf{J}_{\mathrm{field}} = \int \mathbf{r}\times\Big(\frac{\mathbf{E}\times\mathbf{H}}{c^2}\Big) d^3r, \qquad \mathbf{J}_{\mathrm{MDW}} = \int \mathbf{r}\times\rho_{\mathrm{a}}\mathbf{v}_{\mathrm{a}} d^3r. \tag{6}$$

The setup for the experimental measurement of the atomic MDW presented in this work is based on detecting the atomic displacements caused by the transfer of linear momentum with the MDW. Thus, measurements of the angular momentum transfer with the MDW require a different setup.

2.3 Momentum conservation at a material interface

In the MP theory of light, the interface and Abraham force densities are unambiguously linked to the momenta of the incident, reflected, and transmitted fields and the MDW. The conservation law of linear momentum can be written at a general interface between two media as

$$\mathbf{p}_{\mathrm{field,i}} + \mathbf{p}_{\mathrm{MDW,i}} = \mathbf{p}_{\mathrm{field,r}} + \mathbf{p}_{\mathrm{MDW,r}} + \mathbf{p}_{\mathrm{field,t}} + \mathbf{p}_{\mathrm{MDW,t}} + \mathbf{p}_{\mathrm{int}}, \tag{7}$$

where $\mathbf{p}_{\mathrm{field,i}}$ is the momentum of the incident electromagnetic field, $\mathbf{p}_{\mathrm{MDW,i}}$ is the momentum of the incident atomic MDW driven by the optical force, $\mathbf{p}_{\mathrm{field,r}}$ is the momentum of the reflected field, $\mathbf{p}_{\mathrm{MDW,r}}$ is the momentum of the reflected MDW, $\mathbf{p}_{\mathrm{field,t}}$ is the momentum of the transmitted field, $\mathbf{p}_{\mathrm{MDW,t}}$ is the momentum of the transmitted MDW, and $\mathbf{p}_{\mathrm{int}}$ is the recoil momentum taken by a thin interface layer. For normal incidence between lossless media, these momentum components are given in terms of the different components of the optical force density and the momentum $\mathbf{p}_0$ of the field in vacuum as

$$\mathbf{p}_{\mathrm{field,i}} = \frac{\mathbf{p}_0}{n_{\mathrm{g},1}}, \qquad \mathbf{p}_{\mathrm{MDW,i}} = \int\int_{-\infty}^{t} \mathbf{f}_{\mathrm{A,i}} dt' d^3r = \Big(n_{\mathrm{p},1} - \frac{1}{n_{\mathrm{g},1}}\Big)\mathbf{p}_0, \tag{8}$$

$$\mathbf{p}_{\mathrm{field,r}} = -R\frac{\mathbf{p}_0}{n_{\mathrm{g},1}}, \qquad \mathbf{p}_{\mathrm{MDW,r}} = \int\int_{-\infty}^{t} \mathbf{f}_{\mathrm{A,r}} dt' d^3r = -R\Big(n_{\mathrm{p},1} - \frac{1}{n_{\mathrm{g},1}}\Big)\mathbf{p}_0, \tag{9}$$

$$\mathbf{p}_{\mathrm{field,t}} = T\frac{\mathbf{p}_0}{n_{\mathrm{g},2}}, \qquad \mathbf{p}_{\mathrm{MDW,t}} = \int\int_{-\infty}^{t} \mathbf{f}_{\mathrm{A,t}} dt' d^3r = T\Big(n_{\mathrm{p},2} - \frac{1}{n_{\mathrm{g},2}}\Big)\mathbf{p}_0, \tag{10}$$

$$\mathbf{p}_{\mathrm{int}} = \int\int_{-\infty}^{t} \mathbf{f}_{\mathrm{int}} dt' d^3r = [n_{\mathrm{p},1}(1+R) - n_{\mathrm{p},2}T]\mathbf{p}_0. \tag{11}$$

Here, R and T are the conventional power reflection and transmission coefficients of the interface, $n_{\mathrm{p},1}$, $n_{\mathrm{p},2}$, $n_{\mathrm{g},1}$, and $n_{\mathrm{g},2}$ are the phase and group refractive indices of the two media, and $\mathbf{f}_{\mathrm{A,i}}$, $\mathbf{f}_{\mathrm{A,r}}$, $\mathbf{f}_{\mathrm{A,t}}$ are respectively the incident, reflected, and transmitted components of the Abraham force in Eq. (2). The Lorentz force term on free charges and currents in Eq. (2) is zero in a lossless medium.

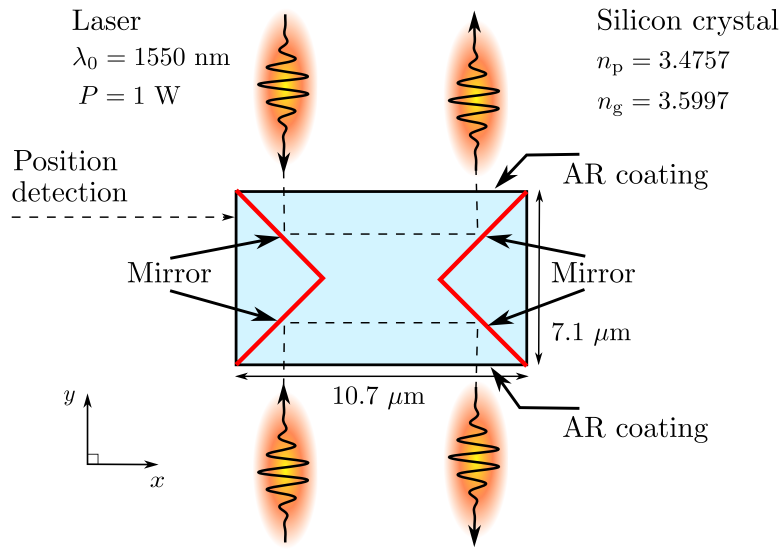

Figure 1. Schematic experimental setup for the measurement of the atomic MDW effect in a microscopic silicon crystal block. The free-standing silicon crystal block has dimensions 10.7 μm $\times$ 7.1 μm $\times$ 3.6 μm and it is assumed to be able to move without friction in the horizontal direction. Anti-reflection (AR) coatings are assumed for the entry and exit interfaces of the crystal. There are two incident 1-W laser beams on the left up and down. Inside the crystal, both laser beams are reflected from two mirror interfaces before they exit the crystal. Position of the crystal block is detected with an external position detection system.

3. SCHEMATIC EXPERIMENTAL SETUP AND THE OCD SIMULATIONS

An illustration of the schematic experimental setup for the measurement of the atomic MDW effect in a microscopic silicon crystal block is presented in Fig. 1. This setup overcomes many challenges that have been present in previously introduced setups and that have made the experimental observation of the MDW effect difficult due to its smallness in comparison with other effects, such as the momentum transfer by absorption and reflections. The present setup also overcomes challenges with elastic relaxation effects while extending possible measurement time scales beyond the time scale of sound waves in the setup geometry.

In the setup in Fig. 1, there are two laser beams incident to the free-standing silicon crystal block on the left up and down. In this arrangement, the net vertical force component experienced by the crystal block is zero as the forces of the beams incident from the up and down cancel each other. Thus, only the horizontal force components contribute to the net movement of the crystal block. Inside the crystal, both laser beams are reflected from two mirror interfaces before they exit the crystal. By the reflection of light, the atoms at the left mirror interfaces experience a force whose horizontal component is to the left while the atoms at the right mirror interfaces experience a corresponding force to the right. However, the net kick experienced by the crystal block due to the transient field of switching on the laser beams is to the left since there is a time difference between the forces experience by the left and right mirror interfaces. In addition to these interface force effects, the Abraham force term in Eq. (2) drives the atomic MDW forward in the crystal, which also contributes to the net displacement of the crystal block. Position of the crystal block is detected with an external position detection system that can be based on any available technology for high-precision position measurements. The dimensions of the silicon crystal block in the setup of Fig. 1 are 10.7 μm in the x direction, 7.1 μm in the y direction, and 3.6 μm in the z direction. For simplicity, anti-reflection coatings are assumed for the interfaces where the laser beams enter and exit the crystal.

Next, we use the OCD model to simulate the propagation of laser beams and the generation of atomic displacements as a result of the optical forces in the silicon crystal of the schematic experimental setup in Fig. 1. We use a vacuum wavelength of $\lambda_0 = 1550$ nm for the two incident laser beams. The heating effects are assumed to be small due to the small absorption coefficient of silicon at this wavelength. We assume the power of 1 W for each of the two incident laser beams, which are focused on the sides of the crystal block in areas with a radius of the order of 1 μm. Thus, the field intensities used in the simulations are well below the irradiation damage threshold of silicon so that the the use of the elastic force density in the OCD model is justified. For the wavelength $\lambda_0 = 1550$ nm, the phase refractive index of silicon is $n_\mathrm{p} = 3.4757$ and the group refractive index is $n_\mathrm{g} = 3.5997$.[31] The dispersion is relatively small, and it is neglected in the present simulations where we use the phase refractive index only.

On the basis of previous OCD simulations,[21,23,24] we use a perturbative approach in which we assume that the back action of the atomic displacements on the field is vanishingly small and can be neglected. We solve the electric and magnetic fields of the laser beams analytically by using Maxwell's equations and assuming that the beams have a Gaussian profile in the transverse directions and a top-hat profile in the longitudinal direction. The transverse Gaussian beam profile is characterized by the waist radius of $w_0 = 0.8$ μm. The optical force density calculated by using these fields via Eq. (2) is then used as an input for the OCD model to describe the coupled field-medium dynamics.

In the OCD simulations, we use the well-known elastic properties of silicon that has an anisotropic cubic lattice structure whose elastic constants in the direction of the (100) plane are $C_{11} = 165.7$ GPa, $C_{12} = 63.9$ GPa, and $C_{44} = 79.6$ GPa.[32] These elastic constants correspond to the bulk modulus of $B = (C_{11} + 2C_{12})/3 = 97.8$ GPa and the shear modulus of $G = C_{44} = 79.6$ GPa. In the present OCD simulations, the (100) lattice plane is assumed to be aligned along the x direction of the geometry in Fig. 1. In addition, in the simulations we use the mass density of silicon, which is $\rho_0 = 2329$ kg/m^3.[33]

Figure 2(a) shows the electromagnetic energy density of the transient fields when the leading edges of the top-hat laser beams are in the middle of the crystal 64 fs after they have entered the crystal. At this instance of time, the left mirror interfaces in Fig. 1 have experienced backward forces due to the reflection of light. This is described by the second term of Eq. (2). In addition, the Abraham force in the third term of Eq. (2) drives the atomic MDW forward in the medium. The horizontal component of the Abraham force at $t = 64$ fs is presented in Fig. 2(b).

Figure 2(c) presents the time dependence of the integrated total (horizontal) optical force F_tot on the crystal block and its contributions associated with the interfaces and the Abraham term in Fig. (2). One can see that the left interface force contribution $F_{\mathrm{int},1}$ is backward while the Abraham force contribution F_A is forward. Both these forces emerge after the laser beams have reached the left mirrors near $t = 20$ fs. The interface force is slightly larger making the total force F_tot to point backward. When the leading edges of the top-hat laser beams are propagating between the mirrors, all total force terms are constant having values $F_{\mathrm{int},1} = -nP_\mathrm{tot}/c = 2.32\times10^{-8}$ N, $F_\mathrm{A} = (n - 1/n)P_\mathrm{tot}/c = 2.13 \times 10^{-8}$ N, and $F_\mathrm{tot} = -(1/n)P_\mathrm{tot}/c = -1.9 \times 10^{-9}$ N, where $P_\mathrm{tot} = 2$ W is the net power of the two laser beams in the crystal. At $t = 90$ fs, the laser beams reach the right mirrors and the right interface contribution $F_{\mathrm{int},2}$ starts to deviate from zero. The total Abraham force term drops to zero and the left interface contribution stays constant. After the leading edges of the laser beams have fully reflected from the right mirrors, the interface forces $F_{\mathrm{int},1}$ and $F_{\mathrm{int},2}$ cancel each other since they are equal, but point in opposite directions. Note that, even though the total integrated Abraham force term is zero, the space- and time-dependent Abraham force is nonzero and continues to drive the atomic MDWs forward in the crystal in accordance with the previous OCD simulations in different geometries.[21–24]

Figure 2(d) depicts the center of mass velocity of the crystal block as a function of time. The center of mass acceleration of the crystal block is simply given by Newton's equation of motion as $a_\mathrm{CM} = F_\mathrm{tot}/M$, where M is the total mass of the crystal block. Using this relation, the center of mass velocity of the crystal block is then given by $v_\mathrm{CM} = \int_{-\infty}^{t} a_\mathrm{CM} dt'$. The center of mass velocity is seen to approach a constant value $v_\mathrm{CM} = -2.86 \times 10^{-10}$ m/s after all the transient field effects of switching on the lasers. Therefore, in longer time scales, the displacement of the medium block practically increases linearly as a function of time as $x_\mathrm{CM} = v_\mathrm{CM}t$. For example, $t = 100$ s after switching on the lasers, the displacement of the crystal block is equal to $x_\mathrm{CM} = -28.6$ nm. This order of magnitude is obviously experimentally measurable. If the Abraham force driving the atomic MDW forward was neglected as done in the well-known Minkowski model, then the displacement of the crystal block would be in the same direction, but it would be as large as $x_\mathrm{CM,Minkowski} = -306$ nm due to the larger magnitude of F_tot during the transient field. Thus, the observation of the smaller magnitude of the atomic displacement predicted above would be a strong evidence for the existence of the Abraham force and the related atomic MDW.

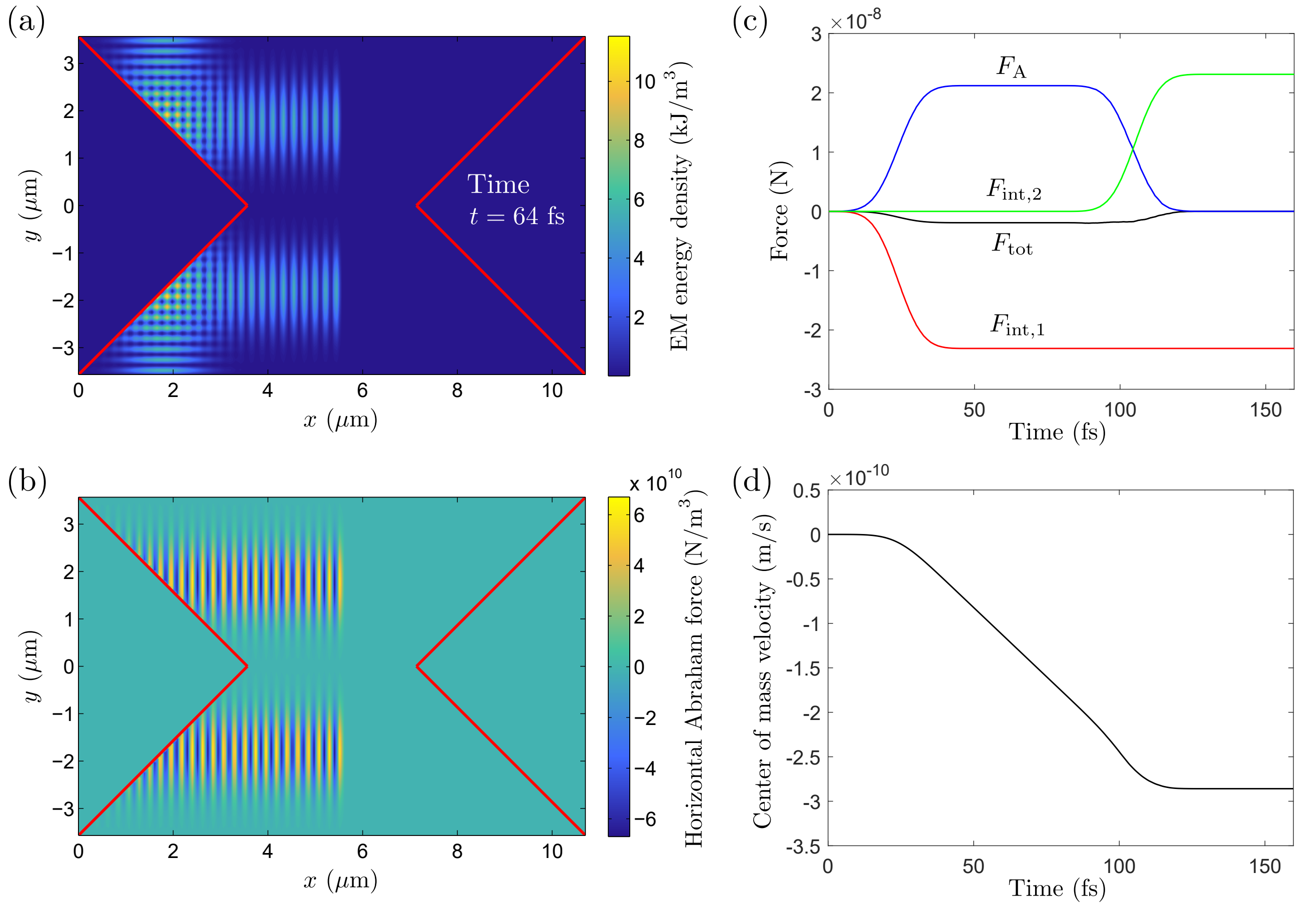

Figure 2. Simulation of the optical forces on the microscopic silicon crystal block under the transient field when the laser beams are switched on. The panel (a) shows the energy density of the electromagnetic field as a function of the position in the plane $z = 0$ μm when the leading edges of the top-hat laser beams are inside the crystal 64 fs after they have entered the crystal. The red lines present the positions of the mirror interfaces. The panel (b) presents the position dependence of the horizontal component of the Abraham force that drives the atomic MDW forward in the crystal. The panel (c) depicts the total force $F_{\rm tot}$, its Abraham force contribution $F_{\rm A}$, the left interface contribution $F_{\rm int,1}$, and the right interface contribution $F_{\rm int,2}$ that are sums of the forces on all medium elements. The panel (d) shows the center of mass velocity of the crystal block as a function of time. The assumed vacuum wavelength of the laser beams is $\lambda_0 = 1550$ nm and the power is 1 W for each of the two beams.

4. CONCLUSIONS

In conclusion, we have used the OCD model to simulate the dynamics of medium atoms in a schematic experimental setup for the measurement of the atomic MDW effect in a silicon crystal. The OCD model allows detailed simulations of the optoelastic dynamics in any material geometry under the influence of the optical force field. For instance, one can model the coupled field-medium dynamics in selected geometries for possible device development needs. The OCD simulations can also be used for more detailed optimization of setups for the experimental verification of the atomic MDW associated with light. Possible obstacles in measuring the atomic MDW effect by using the proposed setup include the possible scattering of light unequally in different directions, which introduces a separate force component that might dominate over the transient field effects in large time scales. The second obstacle is the assumption that the silicon crystal block is free-standing, which may be difficult to realize in long time scales.

ACKNOWLEDGMENTS

This work has been funded by the Academy of Finland under Contract No. 318197 and European Union's Horizon 2020 Marie Skłodowska-Curie Actions (MSCA) individual fellowship DynaLight under Contract No. 846218.

REFERENCES

[1] K. Y. Bliokh and A. Aiello, "Goos-Hänchen and Imbert-Fedorov beam shifts: an overview," *J. Opt.* **15**, 014001 (2013).

[2] K. Y. Bliokh, J. Dressel, and F. Nori, "Conservation of the spin and orbital angular momenta in electromagnetism," *New J. Phys.* **16**, 093037 (2014).

[3] K. Y. Bliokh, F. J. Rodríguez-Fortuño, F. Nori, and A. V. Zayats, "Spin-orbit interactions of light," *Nat. Photon.* **9**, 796 (2015).

[4] L. Du, Z. Man, Y. Zhang, C. Min, S. Zhu, and X. Yuan, "Manipulating orbital angular momentum of light with tailored in-plane polarization states," *Sci. Rep.* **7**, 41001 (2017).

[5] F. Alpeggiani, K. Y. Bliokh, F. Nori, and L. Kuipers, "Electromagnetic helicity in complex media," *Phys. Rev. Lett.* **120**, 243605 (2018).

[6] A. Y. Bekshaev, K. Y. Bliokh, and F. Nori, "Transverse spin and momentum in two-wave interference," *Phys. Rev. X* **5**, 011039 (2015).

[7] J. Lin, J. P. B. Mueller, Q. Wang, G. Yuan, N. Antoniou, X.-C. Yuan, and F. Capasso, "Polarization-controlled tunable directional coupling of surface plasmon polaritons," *Science* **340**, 331 (2013).

[8] K. Y. Bliokh, A. Y. Bekshaev, and F. Nori, "Optical momentum, spin, and angular momentum in dispersive media," *Phys. Rev. Lett.* **119**, 073901 (2017).

[9] K. Y. Bliokh, A. Y. Bekshaev, and F. Nori, "Optical momentum and angular momentum in complex media: from the Abraham-Minkowski debate to unusual properties of surface plasmon-polaritons," *New J. Phys.* **19**, 123014 (2017).

[10] K. Y. Bliokh, A. Y. Bekshaev, and F. Nori, "Extraordinary momentum and spin in evanescent waves," *Nat. Commun.* **5**, 3300 (2014).

[11] G. Molina-Terriza, J. P. Torres, and L. Torner, "Twisted photons," *Nat. Photon.* **3**, 305 (2007).

[12] N. G. C. Astrath, L. C. Malacarne, M. L. Baesso, G. V. B. Lukasievicz, and S. E. Bialkowski, "Unravelling the effects of radiation forces in water," *Nat. Commun.* **5**, 4363 (2014).

[13] H. Choi, M. Park, D. S. Elliott, and K. Oh, "Optomechanical measurement of the Abraham force in an adiabatic liquid-core optical-fiber waveguide," *Phys. Rev. A* **95**, 053817 (2017).

[14] A. Ashkin and J. M. Dziedzic, "Radiation pressure on a free liquid surface," *Phys. Rev. Lett.* **30**, 139 (1973).

[15] A. Casner and J.-P. Delville, "Giant deformations of a liquid-liquid interface induced by the optical radiation pressure," *Phys. Rev. Lett.* **87**, 054503 (2001).

[16] F. A. Schaberle, L. A. Reis, C. Serpa, and L. G. Arnaut, "Photon momentum transfer at water/air interfaces under total internal reflection," *New J. Phys.* **21**, 033013 (2019).

[17] R. V. Jones and J. C. S. Richards, "The pressure of radiation in a refracting medium," *Proc. R. Soc. Lond. A* **221**, 480 (1954).

[18] R. V. Jones and B. Leslie, "The measurement of optical radiation pressure in dispersive media," *Proc. R. Soc. Lond. A* **360**, 347 (1978).

[19] T. Požar and J. Možina, "Measurement of elastic waves induced by the reflection of light," *Phys. Rev. Lett.* **111**, 185501 (2013).

[20] T. Požar, J. Laloš, A. Babnik, R. Petkovšek, M. Bethune-Waddell, K. J. Chau, G. V. B. Lukasievicz, and N. G. C. Astrath, "Isolated detection of elastic waves driven by the momentum of light," *Nat. Commun.* **9**, 3340 (2018).

[21] M. Partanen, T. Häyrynen, J. Oksanen, and J. Tulkki, "Photon mass drag and the momentum of light in a medium," *Phys. Rev. A* **95**, 063850 (2017).

[22] M. Partanen and J. Tulkki, "Mass-polariton theory of light in dispersive media," *Phys. Rev. A* **96**, 063834 (2017).

[23] M. Partanen and J. Tulkki, "Mass-polariton theory of sharing the total angular momentum of light between the field and matter," *Phys. Rev. A* **98**, 033813 (2018).

[24] M. Partanen and J. Tulkki, "Light-driven mass density wave dynamics in optical fibers," *Opt. Express* **26**, 22046 (2018).

[25] M. Partanen and J. Tulkki, "Lorentz covariance of the mass-polariton theory of light," *Phys. Rev. A* **99**, 033852 (2019).

[26] M. Partanen and J. Tulkki, "Lagrangian dynamics of the coupled field-medium state of light," *New J. Phys.* **21**, 073062 (2019).

[27] M. Partanen and J. Tulkki, "Designing the measurement of the atomic mass density wave of a Gaussian mass-polariton pulse in optical fibers," *Opt. Eng.* **58**, 036101 (2019).

[28] M. Partanen and J. Tulkki, "Measuring and engineering the atomic mass density wave of a Gaussian mass-polariton pulse in optical fibers," in *Proc. SPIE 10526, Physics and Simulation of Optoelectronic Devices XXVI*, 105260V, SPIE (2018).

[29] M. Partanen and J. Tulkki, "Angular momentum dynamics of light-driven mass density waves in thin film structures," in *Proc. SPIE 10935, Complex Light and Optical Forces XIII*, 109350B, SPIE (2019).

[30] C. Kittel, *Introduction to Solid State Physics*, Wiley, Hoboken, NJ (2005).

[31] C. Schinke, P. C. Peest, J. Schmidt, R. Brendel, K. Bothe, M. R. Vogt, I. Kröger, S. Winter, A. Schirmacher, S. Lim, H. T. Nguyen, and D. MacDonald, "Uncertainty analysis for the coefficient of band-to-band absorption of crystalline silicon," *AIP Advances* **5**, 067168 (2015).

[32] M. A. Hopcroft, W. D. Nix, and T. W. Kenny, "What is the Young's modulus of silicon?" *J. Microelectromech. Syst.* **19**, 229 (2010).

[33] D. R. Lide, ed., *CRC Handbook of Chemistry and Physics*, CRC Press, Boca Raton, FL (2004).